Electronic Supplementary Material (ESI) for Journal of Materials Chemistry C.

Supporting Information for

Self-assembled Buffer Layer from Conjugated Diblock Copolymers with Ethyleneoxide Side Chains for High Efficiency Polymer Solar Cells

Yueqin Shi[1], Licheng Tan[1], Lie Chen[1], Yiwang Chen[*1,2]

[1]Institute of Polymers/Department of Chemistry, Nanchang University, 999 Xuefu Avenue, Nanchang 330031, China; [2]Jiangxi Provincial Key Laboratory of New Energy Chemistry, Nanchang University, 999 Xuefu Avenue, Nanchang 330031, China

Materials

3-Thiophenemethanol, triethylene glycol monomethyl ether, NBS, methylenechloride, 2,5-dibromo-3-hexylthiophene, sodium bicarbonate, sodium hydroxide, phosphorus tribromide, sodium hydride, anhydrous lithium perchlorate ($LiClO_4$, 99.99%) and [1,3-bis(diphenylphosphino)propane]-dichloronickel (II), 1,2-dichlorobenzene (o-DCB, spectrum pure) and methanol (spectrum pure) were purchased from Alfa Aesar and used as received without any further purification. Tetrahydrofuran (THF) and hexane was dried over sodium. 1M solution of magnesium bromide, toluene and other chemicals were obtained from Shanghai Reagent Co.,Ltd., and used as received. Regioregular P3HT (Mw = 48300 g/mol, head-to-tail, regioregularity > 90%), [6,6]-phenyl-C_{61}-butyric acid methyl ester ($PC_{61}BM$) (99.5% purity), poly(4,8-bis(5-(2-

---

[*] Corresponding author. Tel.: +86 791 83969562; fax: +86 791 83969561. *E-mail address*: ywchen@ncu.edu.cn (Y. Chen).

ethyl-hexyl)-thiophene-2-yl)-benzo[1,2-b:4,5-b']dithiophene-alt-alkylcarbonyl-thieno[3,4-b]thiophene) (PBDTTT-C-T), [6,6]-phenyl-C_{71}-butyric acid methyl ester ($PC_{71}BM$) and MoO_3 were purchased from Rieke Metals, Inc. and Nano-C,. Indium-tin oxide (ITO) glass was obtained from Delta Technologies Limited while PEDOT: PSS (Baytron PAl4083) was purchased from Bayer Inc.

1. Synthesis of 2,5-dibromo-3-thiophenemethanol

3-thiophenemethanol (5.0 g, 4.4×10^{-2} mol) was dissolved in THF (40 mL) in a dried 250 mL round bottom flask wrapped in aluminum foil. The flask was degassed with nitrogen for 15 min before being sealed under a nitrogen atmosphere. NBS (15.6 g, 8.76×10^{-2} mol) was added to the reaction mixture and the reaction was run at room temperature overnight. The solution was filtered to remove residual NBS, then THF was removed by rotary evaporation. The product was dissolved in diethyl ether, then rinsed with 1 M sodium hydroxide solution and water. The organic layer was concentrated and the product was eluted over silica gel using hexane. The solvent was removed by rotary evaporation to yield the desired product as an oily liquid. ^{1}H NMR ($CDCl_3$, δ, ppm): 4.6 (s, 2H) and 6.7 (s, 1H).

2. Synthesis of 2,5-dibromo-3-bromomethylthiophene

2, 5-dibromo-3-thiophenemethanol in dry methylenechloride (100 mL) was added to a 250 mL flask, and sealed under a nitrogen atmosphere. The flask was placed in an ice water bath and the mixture was stirred for 20 min. Phosphorus tribromide (1.73 mL,

1.84×10^{-2} mol) was added dropwise to the solution over a 15 min period. The reaction was run at room temperature for 5 hours, then quenched with sodium bicarbonate solution. The organic solution was passed through a plug of celite, rinsed with water and dried over magnesium sulfate. The solution was filtered and dried using rotary evaporation to yield the product as a light yellow solid. ^{1}H NMR ($CDCl_3$, δ, ppm): 4.8 (s, 2H) and 6.7 (s, 2H).

3. Synthesis of 2,5-dibromo-3-{2-[2-(2-methoxyethoxy)ethoxy]ethoxymethyl} thiophene

Triethylene glycol monomethyl ether (5.0 g, 3.0×10^{-2} mol) was dissolved in THF (125 mL) in a nitrogen bottle and equipped with an addition funnel and septum with nitrogen inlet. Sodium hydride (0.8 g, 3.3×10^{-2} mol) was added and after hydrogen gas evolution had ceased, the flask was sealed under a nitrogen atmosphere. 2,5-dibromo-3-bromomethylthiophene (9.7 g, 2.9×10^{-2} mol) was dissolved in THF (25 mL) and added dropwise to the reaction mixture at room temperature over the course of 10 minutes. Stirring was continued for 4 hours. The mixture was run through a plug of Celite and the solvent was removed by rotary evaporation. The crude product was eluted over silica gel with hexane. The solution was filtered and dried using rotary evaporation to yield the product as a yellow solid. ^{1}H NMR ($CDCl_3$, δ, ppm): 3.3 (s, 3H), 3.5-3.7 (m, 12H), 4.6 (s, 2H), 6.7 (s, 1H)

4. Synthesis of poly(3-hexylthiophene)-block-poly(3-triethylene glycolthiophene)

(P3HT-b-P3TEGT) diblock copolymers [1]

2,5-dibromo-3-hexylthiophene (3.0×10^{-3} mol) and THF (20 mL) were added to a 100 mL flask equipped with a condenser and nitrogen inlet, marked as A solution. 2,5-dibromo-3-{2-[2-(2-methoxyethoxy)ethoxy]ethoxymethyl} thiophene (7.5×10^{-4} mol) and THF (6 mL) were added to another 100 mL flask equipped with a condenser and nitrogen inlet, marked as B solution. A 1 M solution of magnesium bromide (3.1 mL, 3.05×10^{-3} mol) was added to A solution and 1 mL magnesium bromide was add to B solution, then all reactions were refluxed for 2 h. The A flask was cooled to room temperature, and [1,3-bis(diphenylphosphino)propane]-dichloronickel（Ⅱ）(3.6×10^{-2} g, 6.75×10^{-5} mol) was added through a tee. The reaction mixture was stirred at reflux temperature until orange fluorescence was observed. About 10 min later, the P3HT was prepared typically to 99% conversion, then 2-bromo-3-TEG-5-magnesium bromodithiophene (B solution) was added by a tee to the P3HT flask (A solution). mixture was precipitated into methanol. The polymer was filtered and purified by sequential soxhlet extractions using methanol, hexane and chloroform respectively. The chloroform fraction was dried to yield the desired diblock copolymer as a deep purple solid.

5. Synthesis of complexation of poly(3-hexylthiophene)-block-poly(3-triethylene glycolthiophene) (P3HT-b-P3TEGT) chelated with Li^+ ions

P3HT-b-P3TEGT (1 mg) and anhydrous lithium perchlorate ($LiClO_4$) (0.3 mg) salts were dissolved in 1 mL 1,2-dichlorobenzene (DCB):methanol (4:1 volume ratio) solvent. The added Li^+ ions could complex with the triethylene glycol side chains of P3HT-b-P3TEGT polymer chains and drive the polymer chains self-assembled into nanowire morphology [1], which had been reported in our previous work.

Characterizations

The nuclear magnetic resonance (NMR) spectra were collected on a Bruker ARX 600 NMR spectrometer with deuterated chloroform as the solvent and with tetramethylsilane (δ=0) as the internal standard. Gel permeation chromatography (GPC) was used to measure molecular weight distributions with a Breeze Waters system consisting of a Rheodyne injector, a Waters 2414 Refractive Index Detector, a Waters 1515 Isocratic HPLC pump, a Waters column Heater module, and a Styragel columnset, Styragel HT3 and HT4, with tetrahydrofuran as an eluent with a flow rate of 1.0 mL/min and the detector at 40 ºC. The ultraviolet–visible (UV-Vis) spectra of the samples were recorded on a Perkin Elmer Lambda 750s spectrophotometer. The X-ray diffraction (XRD) study of the samples was carried out on a Bruker D 8 Focus X-ray diffractometer operating at 30 kV and 20 mA with a copper target (λ =1.54 Å) and at a scanning rate of 1 ^{o}/min. Atomic force microscopic (AFM) images were measured on a nanoscope III A (Digital Instruments) scanning probe microscope using the tapping mode. XPS studies were performed on a Thermo-VG Scientific ESCALAB 250 photoelectron spectrometer using a monochromated ALKa (1, 486.6 eV) X-ray source. All recorded peaks were corrected for electrostatic effects by setting the C-C component of the C 1s peak to 284.8 eV. The base pressure in the XPS analysis chamber was 2×10^{-9} mbar. For the UPS measurements, He I (21.22 eV) radiation line from a discharge lamp was used, with an experimental resolution of

0.15 eV. All the UPS measurements of the onset of photoemission for determining the work function were done using standard procedures with a -5 V bias applied to the sample. Current-voltage (J-V) characteristics were recorded using Keithley 2400 Source Meter in the dark and under 100 mW/cm^2 simulated AM 1.5 G irradiation (Abet Solar Simulator Sun2000).

Device fabrication and characterization

Inverted solar cells were fabricated on ITO-coated glass substrates. The ITO was cleaned sequentially with acetone, detergent aqueous solution, deionized water and isopropyl alchhol. The cleaned ITO was treated with ultraviolet light for 15-20 min. Then, ZnO solution [2] was spin-coated on the treated ITO. After thermal annealed at 230 ^{o}C for 1 hour, a thin layer (about 150 nm) of P3HT:PC$_{61}$BM (1:1 w/w, 20 mg/mL for P3HT) or PBDTTT-C-T:PC$_{71}$BM (1:1.5 w/w, 10 mg/mL for PBDTTT-C-T, with 3% DIO additive) blending with P3HT-b-P3TEGT or complexation of P3HT-b-P3TEGT:Li$^+$ was spin-cast from its solution in 1,2-dichlorobenzene (DCB) on top of the ZnO layer (25 nm). Finally, a 90 nm Ag layer was deposited following the 6 nm MoO$_3$ layer on the buffer layer surface in a vaccum thermal evaporator. Current-voltage (J-V) characteristics were recorded using Keithley 2400 Source Meter in the dark and under 100 mW/cm^2 simulated AM 1.5 G irradiation (Abet Solar Simulator Sun2000). The active layer area was about 4.0 mm^2.

Measurement of work function of Ag deposited on the active layer surface by Ultraviolet Photoelectron Spectroscopy

To explain the enhancement of V_{oc} and forming of interfacial dipole between Ag and active layer, we used the Ultraviolet photoelectron spectroscopy (UPS) to study the interfacial electronic interaction of Ag on active layer surface covered with complexation of triethylen glycol side chains of P3HT-b-P3TEGT chelated with lithium metal ions (Li^+). The work function [3] was determined by the following equation, work function = $h\nu-(E_{cutoff} - E_{onset})$, where $h\nu$ was incident photo energy (21.2 eV) of He Ⅰ, the high binding energy cutoff (E_{cutoff}) and HOMO region (E_{onset}) were the turing points. The E_{cutoff} was determined by linear extrapolation to zero at the yield of secondary electrons, and the E_{onset} was the onset relative to the Femi level (E_f) of Au (0 eV), where the E_f was determined from the Au substrate.

Surface morphology measurement

Since the morphology of vertical distribution of components in the active layer and the forming of P3HT-b-P3TEGT:Li^+ complexation nanowires as anode interfacial layer were desirable for the bulk heterojunction PSCs, we used atomic force microscopy (AFM) under tapping mode to investigate their morphology.

Space-charge-limited-current (SCLC) mobility measurement

In order to characterize the carrier mobility of modified device, hole-only devices were fabricated with a structure of ITO/PEDOT:PSS/Active layer/MoO_3/Au. The carrier mobility was measured using the SCLC model at low voltage which is described by the following Equation:

$$J=9\varepsilon_0\varepsilon_r\mu V^2/8L^3$$

Where ε_0 is the permittivity of free space (8.85×10^{-12} F.m), ε_r is the dielectric constant of active layer, μ is the mobility of the carrier, V is the applied voltage, and L is the film thickness. The thickness of the BHJ blend for SCLC was about 150 nm measured by AFM and fitting the results to a space-charge-limited form, $J^{0.5}$ versus V.

References:

1. E. Lee, B. Hammer, J.-K. Kim, Z. Page, T. Emrick, R. C. Hayward, *J. Am. Chem. Soc.,* 2011, **133,** 10390.

2. Y. Sun, J. H. Seo, C. J. Takacs, J. Seifter, A. J. Heeger, *Adv. Mater.,* 2011, **23,** 1679.

3. J. H. Seo, A. Gutacker, Y. Sun, H. Wu, F. Huang, Y. Cao, U. Scherf, A. J. Heeger, G. C. Bazan, *J. Am. Chem. Soc.,* 2011, **133,** 8416.

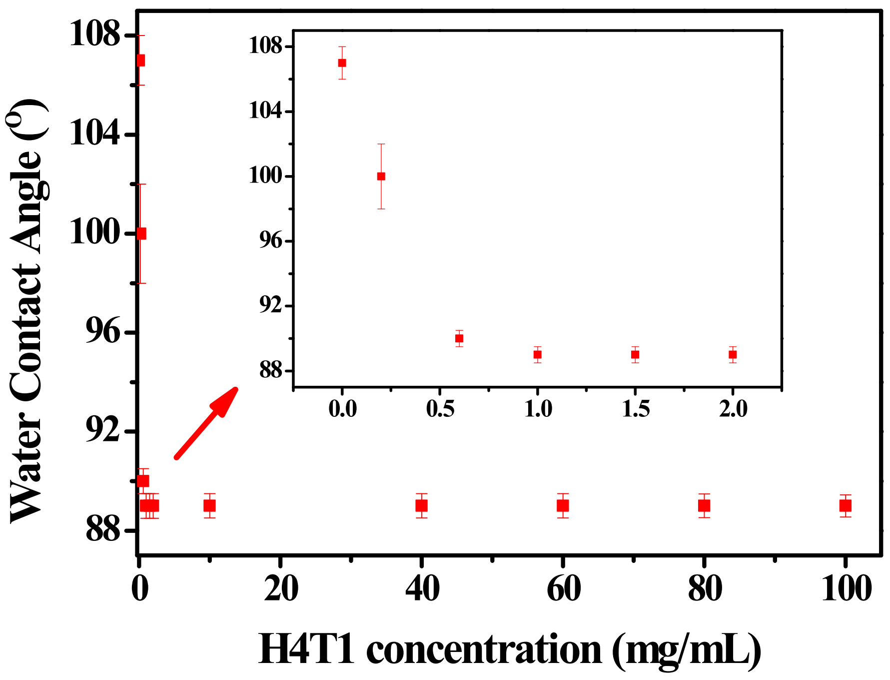

Figure S1. Static water contact angles on the surfaces of PP:H4T1 films plotted as a function of H4T1 concentration in the spin-coating solutions.

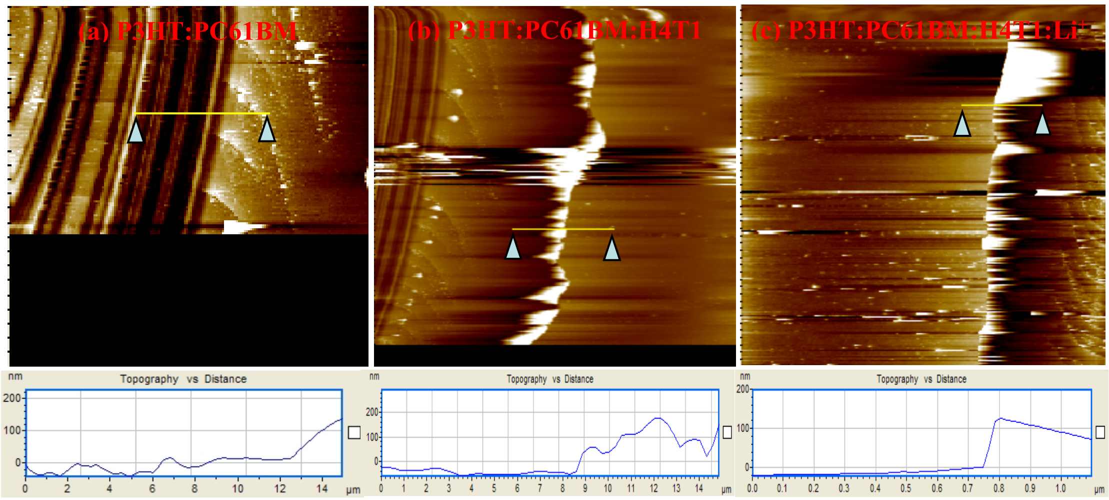

Figure S2. The thickness of P3HT:PC$_{61}$BM, P3HT:PC$_{61}$BM:P3HT-b-P3TEGT and P3HT:PC$_{61}$BM:P3HT-b-P3TEGT:Li^{+} films calculated from AFM measurements.

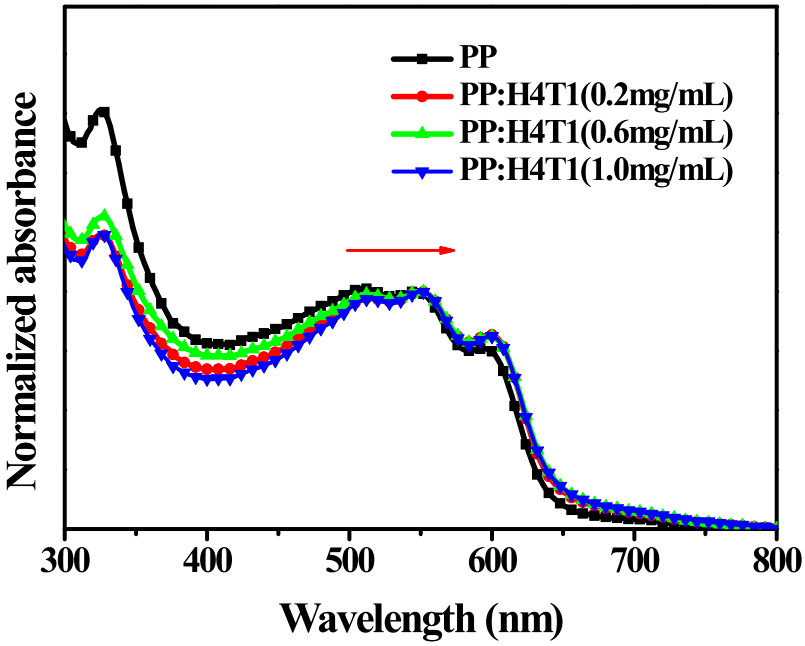

Figure S3. Normalized UV-vis absorption spectra of P3HT:PC_{61}BM with different H4T1 concentration (from 0.0 mg/mL to 1.0 mg/mL).

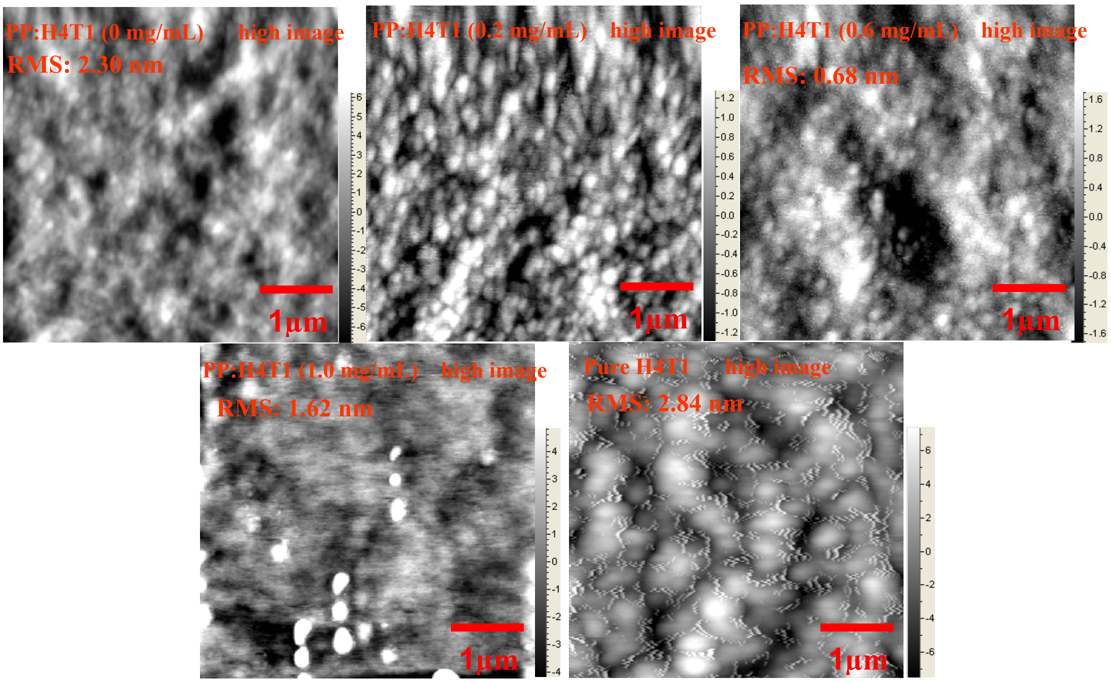

Figure S4. The atomic force microscopy (AFM) high images of P3HT:PC$_{61}$BM with various H4T1 concentration range from 0 mg/mL to 1.0 mg/mL and pure H4T1.

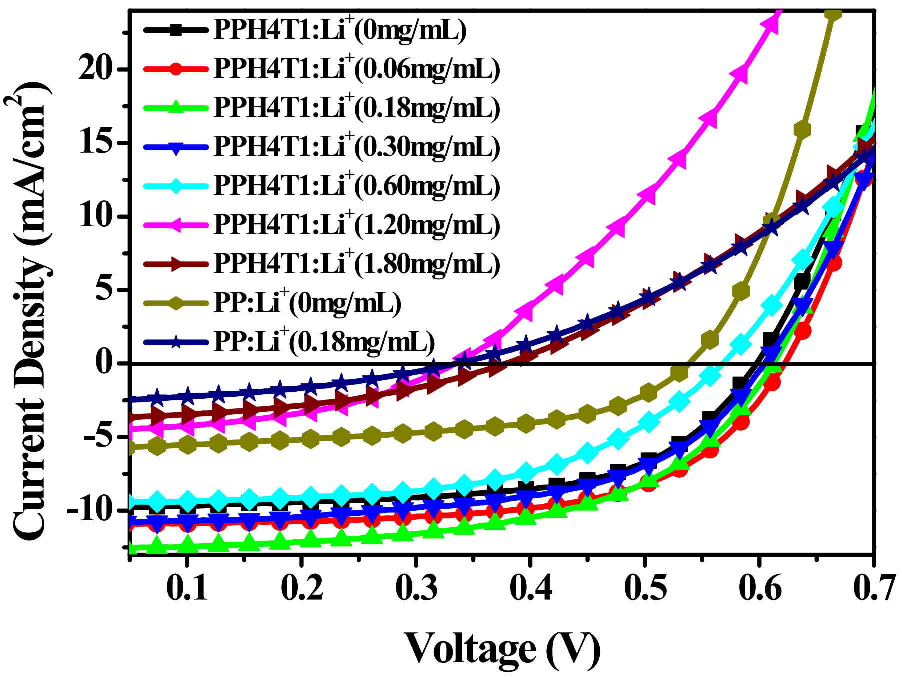

Figure S5. *J-V* curves of the PSCs based on P3HT:PC$_{61}$BM and P3HT:PC$_{61}$BM:H4T1(0.6 mg/mL) with various Li$^+$ concentration under illumination of AM 1.5G, 100 mW/cm^2.

Table S1. Device performance parameters of inverted P3HT:PC_{61}BM:H4T1 (PP:H4T1) solar cells containing various concentrations of Li^+.

Active Layer[a,b,c]	J_{sc} (mA/cm^2)	V_{oc} (V)	FF (%)	PCE
PP:H4T1[d]:Li^+ (0)[e]	9.7	0.59	59	3.38
PP:H4T1[d]:Li^+ (0.06)[e]	9.8	0.59	60	3.47
PP:H4T1[d]:Li^+ (0.18)[e]	9.91	0.59	62	3.6
PP:H4T1[d]:Li^+ (0.3)[e]	8.9	0.58	59	3.05
PP:H4T1[d]:Li^+ (0.6)[e]	8.63	0.57	54	3.0
PP:H4T1[d]:Li^+ (1.2)[e]	4.66	0.34	44	0.7
PP:H4T1[d]:Li^+ (1.8)[e]	3.66	0.38	43	0.6
PP[d]:Li^+ (0)[e]	6.1	0.54	50	1.6
PP[d]:Li^+ (0.18)[e]	2.52	0.34	40	0.3

[a] All values represented averages from fifteen 0.04 cm^2 devices on a single chip. [b] All the devices were annealed at 150 for 10 min before the anode electrode (Ag) evaporation. [c] Device structure: ITO:ZnO(20 nm)/active layer/MoO_3/Ag. [d] PP:H4T1 represented P3HT:PC_{61}BM (1:1 w/w) containing 0.6 mg/mL P3HT4-b-P3TEGT1 with thermal annealing at 150 °C for 10 min and PP represented P3HT:PC_{61}BM (1:1 w/w) with thermal annealing at 150 °C for 10 min. [e] The values in the parentheses presented Li^+ concentrations (mg/mL) in the active layer solutions.

Table S2. Device performance parameters of inverted solar cells with different active layers incorporating triethylene glycol side chains polythiophene (P3HT-b-P3TEGT) with various concentrations or containing complex of P3HT-b-P3TEGT:Li$^+$.

Device[a,b,c]	J_{sc} (mA/cm^2)	V_{oc} (V)	FF (%)	PCE (%)	R_s (Ω·cm^2)	R_{sh} (Ω·cm^2)
ITO/ZnO/PP:H8T1(0.4)[d]/MoO$_3$/Ag	10.2	0.57	56	3.2±0.2	2.7	1178
ITO/ZnO/PP:H8T1(1.2)[d]/MoO$_3$/Ag	9.74	0.59	59	3.4±0.2	2.8	536
ITO/ZnO/PP:H8T1(2.0)[d]/MoO$_3$/Ag	7.81	0.6	58	2.7±0.2	2.9	420
ITO/ZnO/PP:H2T1(0.1)[d]/MoO$_3$/Ag	7.8	0.59	55	2.5±0.2	11.2	1049
ITO/ZnO/PP:H2T1(0.3)[d]/MoO$_3$/Ag	7.54	0.59	58	2.6±0.2	3.2	300
ITO/ZnO/PP:H2T1(0.5)[d]/MoO$_3$/Ag	7.41	0.57	50	2.2±0.2	11.3	769
ITO/ZnO/PP:H8T1(1.2)[d]:Li$^+$(0.18)[e]/MoO$_3$/Ag	11.1	0.60	58	3.9±0.2	1.2	728
ITO/ZnO/PP:H2T1(0.3)[d]:Li$^+$(0.18)[e]/MoO$_3$/Ag	10.9	0.60	60	3.9±0.2	4.1	620
ITO/ZnO/PBP:H8T1(1.2)[d]/MoO$_3$/Ag	15.87	0.77	57	6.9±0.1	3.4	188
ITO/ZnO/PBP:H2T1(0.3)[d]/MoO$_3$/Ag	16.52	0.77	56	7.1±0.1	2.5	211
ITO/ZnO/PBP:H8T1(1.2)[d]:Li$^+$(0.18)[e]/MoO$_3$/Ag	15.86	0.75	54	6.4±0.1	4.8	160
ITO/ZnO/PBP:H2T1(0.3)[d]:Li$^+$(0.18)[e]/MoO$_3$/Ag	16.74	0.75	53	6.6±0.2	3.8	170

[a] All values represented averages from fifteen 0.04 cm^2 devices on a single chip. [b] All the devices were annealed at 150 for 10 min before the anode electrode (Ag) evaporation. [c] Device structure: ITO:ZnO(20 nm)/active layer (150 nm)/Ag. [d] PP represented P3HT:PC$_{61}$BM (1:1 w/w) with thermal annealing at 150 °C for 10 min and PBP represented PBDTTT-C-T:PC$_{71}$BM (1:1.5 w/w) with 3% DIO additive. [d] The values in the parentheses presented the concentrations (mg/mL) of P3HT-b-P3TEGT with different block ratios (H8T1, H4T1 and H2T1) in the active layer solutions. [e] The values in the parentheses presented the concentrations (mg/mL) of Li$^+$ in the active layer solutions. All the MoO$_3$ layers were 6 nm.

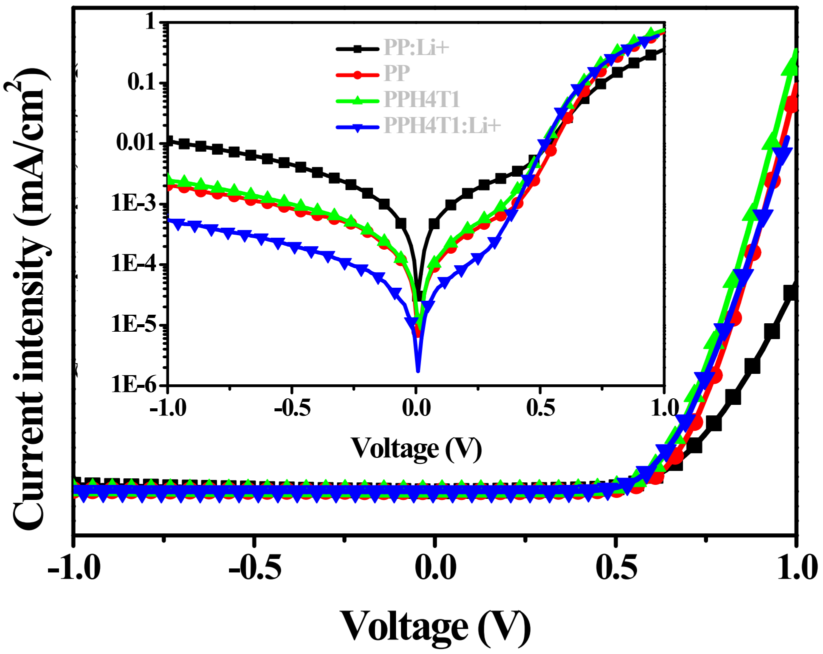

Figure S6. The *J*-*V* curves of device based on active layers with different buffer layers under dark condition.

Table S3. Summary of the carrier mobility of the P3HT:$PC_{61}BM$ device with various HTLs.

Interlayer	Hole mobility[a] ($cm^2/V\cdot s$)
Without interlayer	1.68×10^{-4}
PEDOT:PSS	2.78×10^{-4}
P3HT-b-P3TEGT	5.77×10^{-4}
P3HT-b-P3TEGT:Li^+	1.15×10^{-3}

[a] Hole-only device configuration: ITO/PEDOT:PSS/P3HT:$PC_{61}BM$/MoO_3/Au.

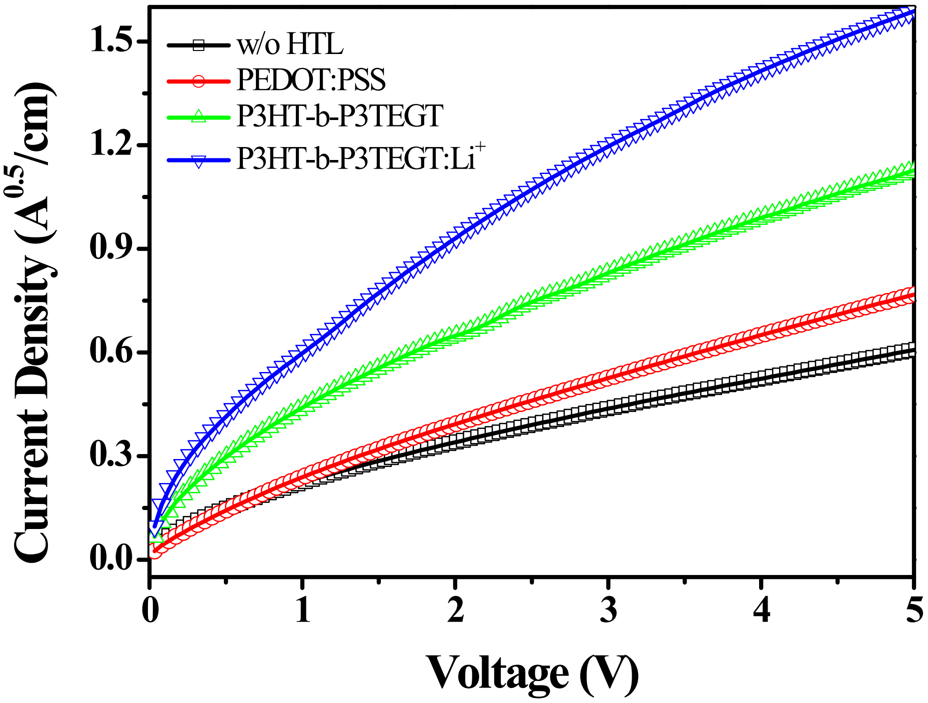

Figure S7. Hole-only device configuration: ITO/PEDOT:PSS/Active layer/MoO_3/Au.

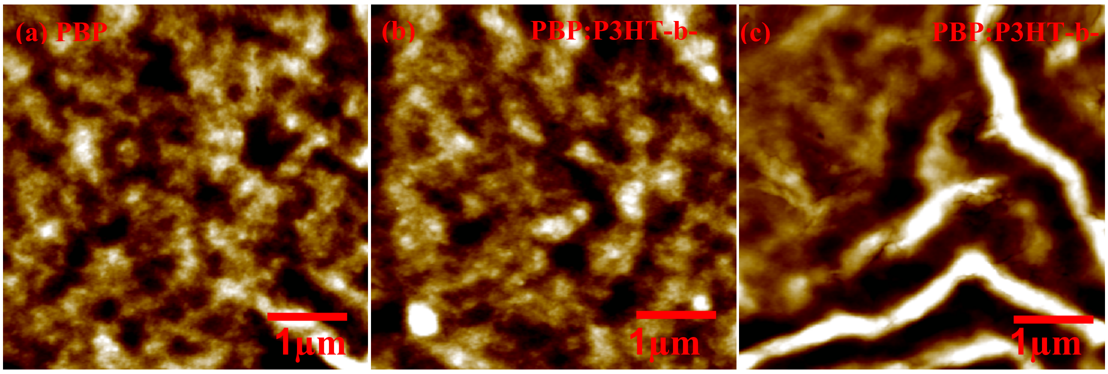

Figure S8. The atomic force microscopy (AFM) high images of (a) PBDTTT-C-T:$PC_{71}BM$ (PBP), (b) PBDTTT-C-T:$PC_{71}BM$:P3HT-b-P3TEGT and (c) PBDTTT-C-T:$PC_{71}BM$:P3HT-b-P3TEGT:Li^+.